JOURNAL OF CATALYSIS 138, 267–282 (1992)

Synthesis Gas Formation by Direct Oxidation of Methane over Pt Monoliths[1]

D. A. HICKMAN AND L. D. SCHMIDT

Department of Chemical Engineering and Materials Science, University of Minnesota, Minneapolis, Minnesota 55455

Received January 27, 1992; revised June 16, 1992

The production of H_2 and CO by catalytic partial oxidation of CH_4 in air at atmospheric pressure has been examined over Pt and Pt–Rh coated monoliths at residence times between 10^{-4} and 10^{-2} sec. With these short contact times, the direct oxidation reaction can be studied independent of reforming reactions. We observe high conversions to H_2 and CO, which strongly suggests that the primary surface reaction is methane pyrolysis, $CH_4 \rightarrow C + 4H$, from which H_2 desorbs and C is oxidized to CO. With room-temperature feeds using air, the optimal feed composition for H_2 and CO occurs between 15 and 20% CH_4 with optimal selectivities of up to $S_{H_2} \sim 0.5$ and $S_{CO} \sim 0.95$ at 80% conversion of the CH_4 at ~1100°C. Increasing the adiabatic reaction temperature by preheating the reactant gases or by using O_2 instead of air improves S_{H_2} to as much as 0.7 for a Pt catalyst and shifts the optimal feed composition toward the stoichiometric feed composition for H_2 and CO production. By examining several catalyst configurations, including Pt-10% Rh woven gauzes and Pt-coated ceramic foam and extruded monoliths, several reaction and reactor variables in producing H_2 and CO have been examined. These experiments show that the selectivity is improved by operating at higher gas and catalyst temperatures, by maintaining high rates of mass transfer through the boundary layer at the catalyst surface, and by using catalysts with high metal loadings. At flow rates high enough to minimize mass-transfer limitations, the gauze, foam monoliths, and extruded monoliths all give similar selectivities and conversions, but with important differences resulting from different catalyst geometries and thermal conductivities.

INTRODUCTION

Much recent research (*1–5*) has been devoted to converting methane to products that are more easily transported and more valuable. Such more valuable products include higher hydrocarbons and the partial oxidation products of methane which are formed by either direct routes such as oxidative coupling reactions or indirect methods via synthesis gas as an intermediate.

Typically, synthesis gas is produced from methane by steam reforming:

$$CH_4 + H_2O \rightarrow CO + 3\,H_2, \quad \Delta H = +49.2\ \text{kcal/mole}. \quad (1)$$

Energy is supplied to drive this endothermic reaction by heating the reactor externally or by adding oxygen to the feed to provide the necessary energy by highly exothermic combustion reactions. A typical steam reformer operates at 15 to 30 atm and 850 to 900°C with an Ni/Al_2O_3 catalyst and a superficial contact time (based on the feed gases at STP) of 0.5 to 1.5 sec (*6*), which corresponds to a residence time of several seconds. The CO/H_2 ratio of the reformer product gases is often modified in a shift reactor which utilizes the water–gas shift reaction:

$$CO + H_2O \leftrightarrow CO_2 + H_2, \quad \Delta H = -9.8\ \text{kcal/mole}. \quad (2)$$

A high temperature water-gas shift reactor (~400°C) typically uses an iron oxide/

[1] This research was partially supported by DOE under Grant DE-FG02-88ER13878-AO2.

0021-9517/92 $5.00

chromia catalyst, while a low-temperature shift reactor (~200°C) uses a copper-based catalyst. Both low- and high-temperature shift reactors have superficial contact times (based on the feed gases at STP) greater than 1 sec (*7*).

An alternate approach for producing synthesis gas from methane is the direct oxidation of CH_4:

$$CH_4 + \frac{1}{2}O_2 \rightarrow CO + 2H_2, \quad \Delta H = -8.5 \text{ kcal/mole.} \quad (3)$$

While this reaction is exothermic, the oxidation reactions which produce H_2O from methane are much more exothermic,

$$CH_4 + \frac{3}{2}O_2 \rightarrow CO + 2H_2O, \quad \Delta H = -124.1 \text{ kcal/mole,} \quad (4)$$

$$CH_4 + 2O_2 \rightarrow CO_2 + 2H_2O \quad \Delta H = -191.8 \text{ kcal/mole.} \quad (5)$$

Oxidation reactions are much faster than reforming reactions, suggesting that a single-stage process for syngas generation would be a viable alternative to steam reforming.

The objective of the research described here is to explore synthesis gas generation by direct oxidation of CH_4, reaction (3). A reactor giving complete conversion to a 2/1 mixture of H_2 and CO would be the ideal upstream process for the production of CH_3OH or for the Fischer–Tropsch process. As discussed above, currently implemented or proposed processes utilize a combination of oxidation and reforming reactions to generate synthesis gas from CH_4 and O_2. In this work, we seek a faster, more efficient route of syngas generation in which H_2 and CO are the *primary products* of CH_4 oxidation. It is expected that this may be difficult because the reactions $H_2 + O_2 \rightarrow H_2O$ and $CO + \frac{1}{2}O_2 \rightarrow CO_2$ are extremely fast (*8–10*), either heterogeneously or homogeneously, while CH_4 activation is quite slow except at high temperatures.

Most fundamental studies have dealt with the $CH_4 + O_2$ reaction system in excess O_2 and at lower temperatures (*11–15*). However, the topic of syngas by oxidation of CH_4 has been considered recently from an engineering perspective. One proposed direct oxidation reactor (*1*) consists of catalytic metals (Pt and Pd) supported by an alumina washcoat on several cordierite extruded monoliths about 1 m in diameter which are stacked in series to give a total reactor length of about 2 m. This reactor requires residence times of ~0.04 sec to obtain essentially complete conversion of CH_4.

Another proposed direct oxidation reactor uses natural gas and air at atmospheric pressure and 800 to 1000°C over an Ni/Al_2O_3 catalyst (*2*). This reactor operates adiabatically, implementing an unsteady-state mode of operation in which the flow direction is periodically reversed to maintain high temperatures. At the entrance to the reaction zone, the combustion reactions (4) and (5) occur, resulting in a peak temperature of 950°C. Downstream from this zone, steam reforming and CO_2 reforming convert most of the remaining CH_4 to syngas. Residence times of about 0.25 sec are required to give H_2 and CO selectivities of 75 to 85% and 75 to 95%, respectively, with 85 to 97% conversion of the methane feed.

This sequence of total oxidation reactions followed by reforming reactions was also used in experiments which examined the oxidation state and phase composition of the Ni/Al_2O_3 catalyst as a function of axial position in the catalyst bed (*3*). In these atmospheric pressure experiments, the oxidation of methane was studied at temperatures between 450 and 900°C. Contact times of about 0.1 sec were required to give equilibrium yields of H_2 and CO.

Experiments over mixed metal oxides of ruthenium (*4*) and over a variety of supported transition metals (*5*) also showed that nearly equilibrium yields of H_2 and CO could be obtained at temperatures above ~750°C. These authors also attributed the

high H_2 and CO selectivities to a sequence of total oxidation of a fraction of the initial CH_4 followed by the reforming and shift reactions.

In this paper, we present results from a methane direct oxidation reactor for residence times between 10^{-4} and 10^{-2} sec. For this work, methane oxidation (using air as the oxygen source) was studied over Pt-10% Rh gauze catalysts and Pt-coated (or Pt/Rh-coated) foam and extruded monoliths at atmospheric pressure, and the reactor was operated autothermally rather than at thermostatically controlled catalyst temperatures. By comparing the steady-state performance of these different catalysts at such short contact times, the influence of several key parameters on the direct oxidation of methane to synthesis gas can be examined independent of the slower reforming reactions.

We note that it is quite difficult to measure kinetics and selectivities of combustion reactions such as methane oxidation because the reactions are so fast and exothermic. Rates can only be measured versus temperature by lowering the pressure to <1 Torr so that reaction heat does not control the catalyst temperature. Reactions on wires, foils, or single crystals then easily become flux limited and have high conversions at the shortest attainable residence times for complete mixing (>1 sec). While rates have been obtained under these conditions (*11*), their extrapolation to atmosphere pressure is of dubious relevance. In addition, mass-transfer limitations, which are eliminated at low pressures, are invariably encountered in an atmospheric pressure flow reactor (*16*). Thus, our use of an adiabatic, atmospheric pressure reactor both allows us to determine the conversion and selectivity and also is a major measurement from which to determine reaction kinetics and mechanisms.

APPARATUS AND PROCEDURE

The reactor consisted of a quartz tube with an inside diameter of 18 mm which held the monolith or gauze pack. To better approximate adiabatic operation, the catalyst was immediately preceded and followed by inert alumina monoliths which acted as radiation shields, and the outside of the tube at the reaction zone was usually insulated. Bypass of the reactant gases around the annular space between the catalyst sample and the quartz tube was minimized by sealing the catalyst sample with a high temperature alumina-silica cloth.

Gas flow into the reactor was controlled by mass flow controllers which had an accuracy of ±0.01 slpm (standard liters per minute) for CH_4 and ±0.05 slpm for air. The feed flow rates ranged from 2 to 5 slpm total flow, corresponding to 13 to 33 cm/sec superficial velocity (i.e., the velocity of the feed gases upstream from the catalyst) at room temperature and atmospheric pressure. In all experiments, the reactor pressure was maintained at 1.4 atm. Product gases were fed through heated stainless steel lines to a sample loop in an automated gas chromatograph. The GC analysis was performed using two isothermal columns (80°C) in series. Carbon dioxide was separated from the H_2, O_2, N_2, CH_4, and CO by a Porapak T column. The remaining species were separated in a Molecular Sieve 5A column. Since an He carrier gas was used, the H_2 was transferred from the He stream to an N_2 carrier gas before being fed to the thermal conductivity detector. When necessary, a second GC analysis using a temperature programmed Hayesep R column was used to separate and detect small hydrocarbons (such as ethylene and ethane) and H_2O.

For quantitative determination of the concentrations, standards were used for all species except perhaps H_2O, which could be obtained from an oxygen atom balance. In order to convert the product gas concentrations to molar quantities for a given feed basis, the mole number change due to the chemical reactions was calculated using the measured N_2 concentration. Since N_2 is an inert in this system, the ratio of product gas to feed gas moles was inversely proportional to the ratio of product gas N_2 concentration

to feed gas N_2 concentration. The product gas carbon and hydrogen atom balances typically closed to within ±5%, and individual species concentrations were measured with a reproducibility of ±0.2%.

Temperatures were monitored using thermocouples or an optical pyrometer. One or more thermocouples were inserted from the front or the rear of the quartz tube. Generally, the gas temperatures in the feed and product streams were measured by placing thermocouples in one of the center channels of the inert monolith immediately before or after the catalytic monolith or gauze. Product gas temperatures were the primary data taken in these experiments. Since the downstream thermocouples were placed inside the radiation shields just after the catalyst sample, corrections for radiation effects on the thermocouple were not necessary since the gas and surface temperatures are all equilibrated at the exit of the catalyst sample.

For the reactor preheat experiments, the feed gas temperatures were measured based on a fixed reactor preheater power input for a given feed flow rate without reaction. Thus, the preheat temperature was calibrated against the preheat power input before igniting the catalyst. Obviously, the back-mixing of energy by radiation and conduction to the upstream radiation shield during reaction increased the temperature of the feed gases at the upstream end of the catalyst above the reported preheat temperature. In these experiments, however, the intent was to determine the effect of increasing the adiabatic temperature of the reactor, not to measure the actual temperature of the gases as they reached the upstream side of the catalyst.

An optical pyrometer was used in experiments where a constant surface temperature was required. The pyrometer was calibrated for a given catalyst by making simultaneous measurements with a thermocouple. Because these catalysts do not have flat, uniform surfaces, the temperatures readings obtained with the pyrometer were not assumed to be accurate. The pyrometer was only used to make certain that the surface temperature did not change during an isothermal experiment.

In these experiments, the reactions were ignited by preheating the gases to the heterogeneous ignition temperature for the feed mixture. Since CH_4–air mixtures require feed gas temperatures of ~600°C for heterogeneous ignition, while NH_3–CH_4–air mixtures ignite at ~200°C (*17*), NH_3 was added to the feed gases until heterogeneous reactions were ignited. Then the NH_3 flow was stopped and the reactor was operated autothermally.

The reactor was operated at a steady state temperature which is a function of the heat generated by the exothermic reactions and the heat losses from the reactor. The overall heat generation rate due to chemical reaction (Q_{gen}) is equal to the heat energy (energy/time) carried in the product gases (Q_{prod}) and the rate of energy loss from the reactor by conduction, convection, and radiation (Q_{loss}):

$$Q_{gen} = Q_{prod} + Q_{loss}. \qquad (6)$$

Since Q_{loss} for a given reactor temperature and catalyst is at a fixed rate per time, and Q_{gen} increases with total flow, the reactor approaches the limit of adiabatic operation ($Q_{prod} \gg Q_{loss}$) as the total flow rate of gases increases. The autothermal temperatures observed in experiments at 4 to 5 slpm total flow were estimated to be 50 to 100°C less than the adiabatic temperatures with insulation and ~200°C less than the adiabatic temperatures without insulation.

MONOLITHS

In these experiments, three types of catalysts were studied: metal gauzes, metal-coated foam monoliths, and metal-coated extruded monoliths. The gauze catalysts were 40 mesh (40 wires per inch) or 80 mesh Pt-10% Rh woven wire samples which were cut into 18-mm diameter circles and stacked

together to form a single gauze pack 1 to 10 layers thick. They were typically sandwiched between two extruded ceramic supports. These gauze catalysts are used industrially in the oxidation of NH_3 to NO for nitric acid production and in the synthesis of HCN from NH_3, CH_4, and air.

The foam monoliths were α-Al_2O_3 samples with an open cellular, sponge-like structure. We used samples with nominally 30 to 50 pores per inch (ppi) which were cut into 17-mm diameter cylinders 2 to 20 mm long. A coating of Pt or Pt–Rh was then applied directly to the alumina by a technique involving an organometallic deposition. Relatively high loadings of noble metals were used. The foam monolith samples used in this work had loadings which varied from 12 to 20 wt% noble metal. Scanning electron microscopy (SEM) micrographs of these catalysts before and after use revealed that the catalyst formed large crystallites on the support with metal covering a significant fraction of the support surface.

The cordierite extruded monoliths, having 400 square cells/in^2, were similar to those used in automobile catalytic converters. However, instead of using an alumina washcoat as in the catalytic converter, these catalyst supports were loaded directly with 12 to 14 wt% Pt in the same manner as the foam monoliths. Because these extruded monoliths consist of several straight, parallel channels, the flow in these monoliths is laminar (with entrance effects) at the flow rates studied.

For all types of monoliths, experiments were run on many samples. We show results from only a few of these, but the results were nominally reproducible for all samples.

REACTION STOICHIOMETRY AND EQUILIBRIUM

Before presenting the results of our experiments, we briefly describe the essential roles of stoichiometry and thermodynamics in this system.

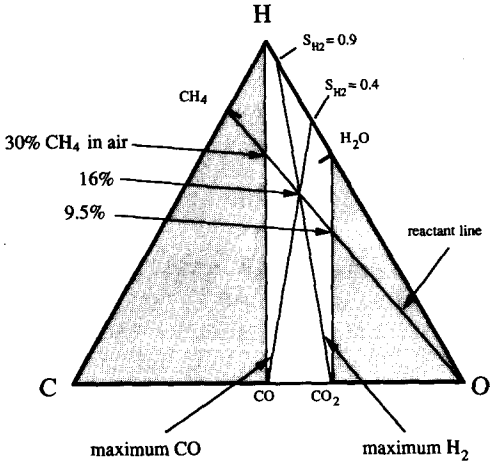

FIG. 1. A ternary composition diagram of the C–H–O system. Shown on the diagram is the range of allowable selectivities for complete conversion of an initial feed containing 16% CH_4 in air.

The performance is governed by the conversions of CH_4 and O_2 and the selectivities in producing H_2 and CO:

$$S_{H_2} = \frac{1}{2}\frac{F_{H_2}}{F_{CH_4in} - F_{CH_4out}} = \frac{F_{H_2}}{F_{H_2} + F_{H_2O}} \quad (7)$$

and

$$S_{CO} = \frac{F_{CO}}{F_{CH_4in} - F_{CH_4out}} = \frac{F_{CO}}{F_{CO} + F_{CO_2}}, \quad (8)$$

where F_i is the molar flow rate of species i. Because there are only three atomic species in this reaction system (C, H, and O), if H_2, H_2O, CO, and CO_2 are the only reaction products, these two selectivities are related by the equation

$$S_{H_2} + \frac{1}{2}S_{CO} = 2 - \frac{F_{O_2in} - F_{O_2out}}{F_{CH_4in} - F_{CH_4out}}. \quad (9)$$

The role of stoichiometry in this system is illustrated by the ternary plot of Fig. 1. For any reaction where CH_4 and O_2 are the only reactant species in the feed, the atomic

composition of the mixture is represented by a point located on the reactant line shown in the figure. The unshaded area represents the accessible region of H_2, H_2O, CO, and CO_2 compositions corresponding to total conversion of between 9.5% (H_2O and CO_2) and 29.6% (H_2 and CO) CH_4 in air or between 33.3 and 66.7% CH_4 in O_2. The composition point corresponding to 16% CH_4 in air is designated in this example. If the methane and oxygen at this composition are completely converted to a mixture of CO, CO_2, H_2, and H_2O, the composition of the product gases can be described by *straight lines that pass through this point*. Two limiting product lines are depicted in the figure, one for maximum CO and one for maximum H_2. This, for a given reacted feed composition, an increase in the selectivity of CO formation must result in a corresponding decrease in the H_2 selectivity. The lightly shaded region indicates the inaccessible compositions for this feed composition.

Obviously, the stoichiometry of reaction (3) suggests that the ideal synthesis gas reactor should operate at a CH_4/O_2 mole ratio of 2/1 (29.6% CH_4 in air) if total conversion of the reactants occurs. At high enough temperatures, this mixture is completely converted to H_2 and CO at thermodynamic equilibrium. Below about 1000°C, the equilibrium mole fraction of carbon becomes significant. Hence, a reactor must be maintained above 1000°C to avoid carbon formation. In experiments at lower temperatures, the formation of carbon can have an adverse effect on the catalyst as time progresses (*2*).

For initial compositions of between 9.5 and 29.6% CH_4 in air, stoichiometry requires that some H_2O and CO_2 exist in an equilibrium mixture. For all such initial compositions above 1000°C, essentially only CO, CO_2, H_2, and H_2O remain in the equilibrium mixture. The H_2 and CO selectivities change with temperature because of the water–gas shift equilibrium. As the temperature increases, this equilibrium shifts toward the formation of more H_2O and CO according to reaction (2), but H_2 and CO are still the dominant equilibrium species for rich $CH_4 + O_2$ feeds.

RESULTS

Role of Temperature

We first show results for a typical experiment using a Pt-coated (11.6% by weight), 50-ppi alumina foam monolith 7 mm in length. In Fig. 2, measured product gas compositions, selectivities, and temperatures are shown as a function of feed composition and preheat temperature. The mass flow rate was maintained at 5 slpm, which corresponds to a superficial velocity of 100 cm/sec (assuming a gas temperature of 1000°C and a void fraction of 0.85) and thus a residence time of ~7 msec. Similar behavior was also observed in identical experiments performed with 1 to 10 layers of Pt-10% Rh gauze catalyst.

For a given feed temperature, CH_4 conversion is essentially complete (~95%) for feed CH_4 compositions sufficiently lean in CH_4 (23% at 460°C, 21% at 300°C, and 19% at 25°C). Near this breakthrough point, the H_2 and CO concentrations are at their maxima. Above this, the CH_4 breakthrough increases dramatically, while the O_2 conversion remains complete for all compositions. The CH_4 breakthrough occurs because all of the O_2 has been consumed early in the reactor. This is because some of the CH_4 is converted to H_2O and CO_2 instead of forming only H_2 and CO, leaving no O_2 to react with the remaining CH_4. As the ideal feed composition (29.6% CH_4) is approached from leaner compositions, the CH_4 breakthrough increases drastically. In fact, for feed compositions richer than the CH_4 breakthrough point, the O_2/CH_4 conversion ratio actually increases as the O_2/CH_4 feed ratio decreases. In other words, while the fraction of CH_4 in the feed is increased, the overall molar rate of CH_4 conversion actually decreases, while the O_2 conversion remains complete. Thus, the H_2 and CO selectivities are optimal near the CH_4 breakthrough point.

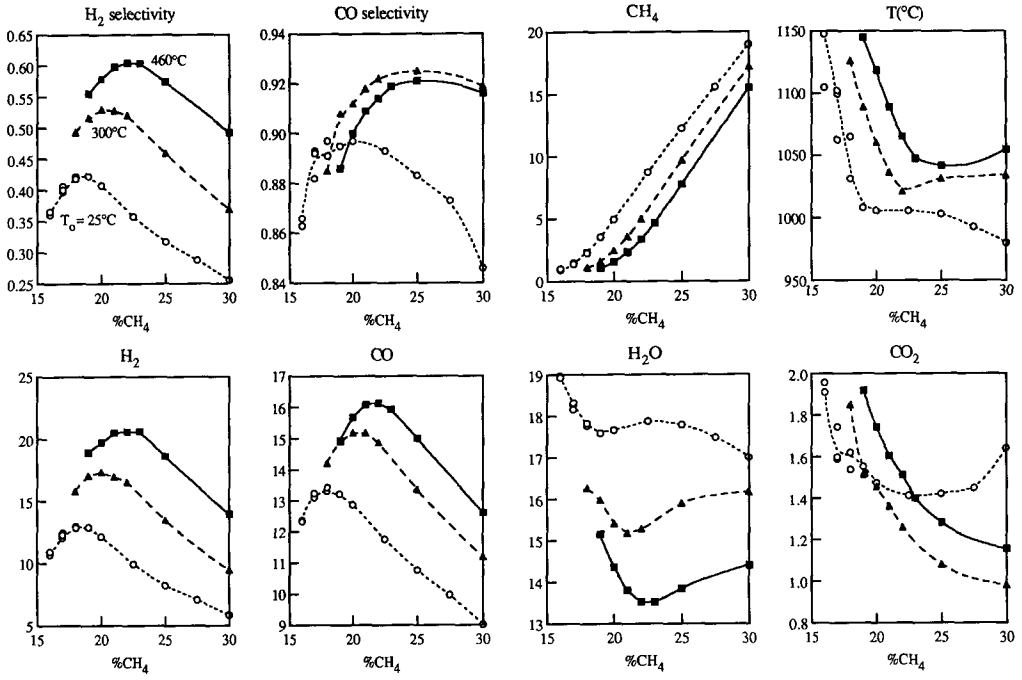

FIG. 2. Molar compositions (based on 100 moles feed gases), selectivities (defined in Eqs. (7) and (8)), and product gas temperatures for CH_4 oxidation over a 7-mm long, 12-wt% Pt, 50-ppi foam monolith with 4 slpm of feed gases and three different feed gas temperatures (○ = 25°C, ▲ = 300°C, and ■ = 460°C).

As the feed CH_4 concentration increases from the lean side of the breakthrough point, the increase in the H_2 and CO selectivities results in decreasing product gas temperatures since the formation of these species is much less exothermic than the formation of H_2O and CO_2.

On the fuel-rich side of the breakthrough point, the temperature levels off just above 1000°C as the heat generated by the formation of H_2O and CO_2 becomes relatively independent of the feed composition. It is interesting to note that the selectivities decrease and the CH_4 breakthrough increases at the same point where the product gas temperature levels off. This is very near the temperature (~1000°C) at which equilibrium graphite forms. This may indicate that the surface cokes when the temperature falls too low and that this slows CH_4 consumption, causing a decrease in the partial oxidation selectivity for both products.

Increasing the temperature of the feed gases shifts the CH_4 breakthrough point and the maxima in H_2 and CO selectivities to richer CH_4 compositions. In addition, the optimal H_2 selectivity increases from about 43 to 60% when the feed is preheated to about 460°C, while the optimal CO selectivity remains fairly constant (>80%). One should note that a difference in feed gas temperatures of 435°C results in a *maximum* difference in product gas temperature of only 150°C. Preheating increases the selectivity of H_2 and CO formation, resulting in a lower adiabatic temperature rise for a given feed composition.

From these data, it is apparent that the primary hurdle to achieving the perfect reactor operation described by reaction (3) involves the selective oxidation of CH_4 to H_2 and CO only. If H_2O and CO_2 are formed, the amount of available O_2 is obviously reduced accordingly. From stoichiometry,

this results in unreacted CH_4 in the product gases since the reforming reaction is too slow to consume this methane at these short residence times.

Equivalently, one can say that, since CO, CO_2, H_2, and H_2O are essentially the only reaction products, perfect selectivities can be obtained only if the molar O_2/CH_4 conversion ratio is 0.5. As shown in Fig. 2, preheating the feed gases decreases this ratio for a given feed composition, and the optimal feed composition shifts from 18 to 23% CH_4. This trend suggests that additional preheating above 460°C would further improve reactor performance. Also, the adiabatic reactor would operate 50 to 100°C hotter, so that a large reactor should have higher selectivities than those shown here.

In addition to preheating the reactor, the adiabatic temperature can also be increased by using O_2 instead of air. Without the N_2 diluent, the adiabatic temperature rise for a given conversion is significantly higher. In experiments using O_2 with the same catalyst as in Fig. 2, we obtained optimal selectivities of $S_{H_2} \sim 0.7$ and $S_{CO} \sim 0.95$ for a room-temperature feed at a feed molar ratio of $CH_4/O_2 = 1.7$ (equivalent to 26.3% CH_4 in air) and an adiabatic temperature of ~1130°C.

Role of Mass Transfer and Gas Phase Reactions

Figure 3 illustrates the effect of gas flow rate on selectivity and conversion. For these experiments, 10 layers of Pt-10% Rh gauze were used and the surface temperature of the first layer of gauze was kept constant by heating or cooling the reactor tube in order to decouple the effects of temperature and velocity on selectivity. In other words, since the catalytic reaction rates are expected to depend strongly on the surface temperature, the effect of external mass transfer (which changes with velocity) was isolated from the effect of reaction kinetics. The first gauze was kept isothermal since another experiment (Fig. 4) demonstrated that most of the reaction occurs on the first layer of gauze.

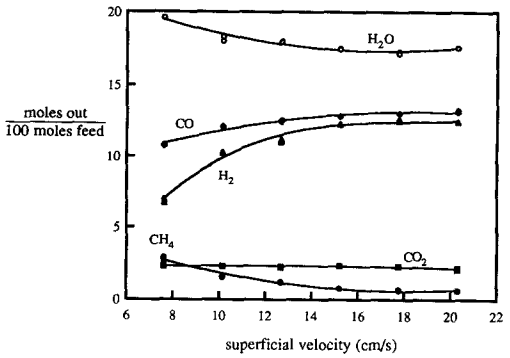

FIG. 3. Effect of flow velocity on product gas composition for CH_4 oxidation over 10 layers of 40 mesh Pt-10% Rh gauze. The feed contained 16% CH_4 in air and the front layer of gauze was maintained at 1227 ± 5°C.

As shown, although increasing the gas velocity decreases the residence time of the gases, the conversion of CH_4 *actually increases with increasing flow rates.* In addition the selectivities of H_2 and CO formation increase significantly with increasing flow rates. At all flow rates used, all of the available O_2 is consumed. This change in reaction selectivity and conversion can be explained by a simple model which accounts for the effect of external mass transfer on reaction selectivity (*16*).

Because of the relatively high temperature (1227°C) and pressure (1.4 atm) in this experiment, one might expect gas phase reactions to be significant. If gas phase production of CO_2, H_2O, and hydrocarbons were competing with the heterogeneous reactions, increasing the flow velocity at a fixed temperature would decrease the residence time of reactant species in the boundary layer. Thus, the rate of the mass-transfer-limited surface reactions would increase relative to the gas phase reactions. Experiments examining methane oxidation in empty quartz tubes (*18*) have shown that gas phase reactions can be significant at temperatures as low as 650°C, with C_2H_4 and C_2H_6 being produced in reasonable quantities along with CO and CO_2. In our experiments, we only observe at most small quan-

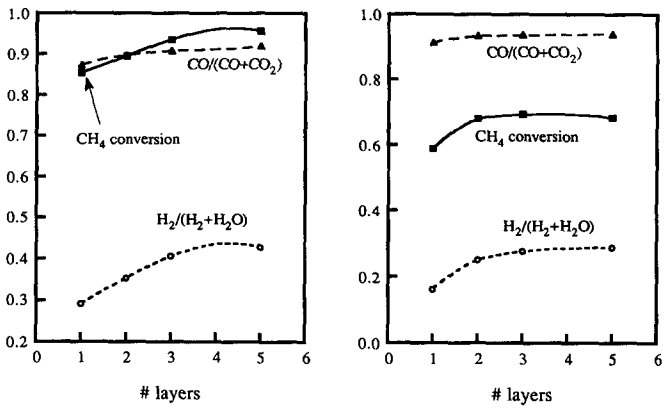

FIG. 4. Variation in selectivities (defined in Eqs. (7) and (8)) and CH_4 conversion with the number of layers of 40 mesh Pt-10% Rh gauze at 5 slpm total flow. Feed compositions were 17% (left panel) and 20% (right panel) CH_4 in air.

tities (<0.5 mole%) of ethane and ethylene in the product gases.

Variation of Number of Gauzes

The selectivities and conversions were also studied as a function of the gauze pack thickness by using a gauze catalyst in which the number of gauzes was varied from 1 to 5 at a constant gas flow rate. (The contact time with a single layer of gauze in these experiments is less than 10^{-4} sec.) When adding an additional gauze layer, we were careful to orient it such that it was not directly aligned with the previous layer. Thus, the addition of a second layer not only increases the residence time, but also decreases the effective channel diameter or spacing between wires. This decrease in effective channel diameter will result in an increase in the mass transfer coefficient by reducing the average boundary layer thickness.

For a total flow rate of 5 slpm with 17% CH_4 in air, all of the O_2 is consumed with even one layer of gauze. However, as the number of layers was increased, the selectivities and CH_4 conversion increased until additional layers resulted in no significant change in the product composition. Thus, *essentially all of the reactions occurred within the first three layers of gauze.* The rate of methane steam reforming should not be significant at these short residence times since the additional fourth and fifth layers do not increase the CH_4 conversion. Equilibrium calculations show that product distributions are far from water–gas shift or reforming equilibrium.

Comparison of Monoliths

Figures 5a–5c show the product selectivities and reactant conversions for two different foam monoliths, an extruded monolith, and a gauze. These experiments were all performed at high flow rates (a mass flow rate of 4 to 5 slpm) to minimize the effect of external mass transfer on selectivity. In all cases, all of the O_2 was consumed. From these data, we can make several important observations.

First, a 50-ppi foam, coated with a 1/1 Pt/Rh weight ratio (9.9 wt% each of Pt and Rh), gives higher CH_4 conversions than the 12-wt% Pt-coated 50-ppi sample. The sample containing Rh gives a higher H_2 selectivity, while the CO selectivity is slightly lower. This result is consistent with other evidence (*19*) which indicates that Rh oxidizes CO to CO_2 faster than Pt.

Second, a 12-wt% Pt extruded cordierite monolith, which has laminar flow, gives similar conversions and selectivities to the 50-

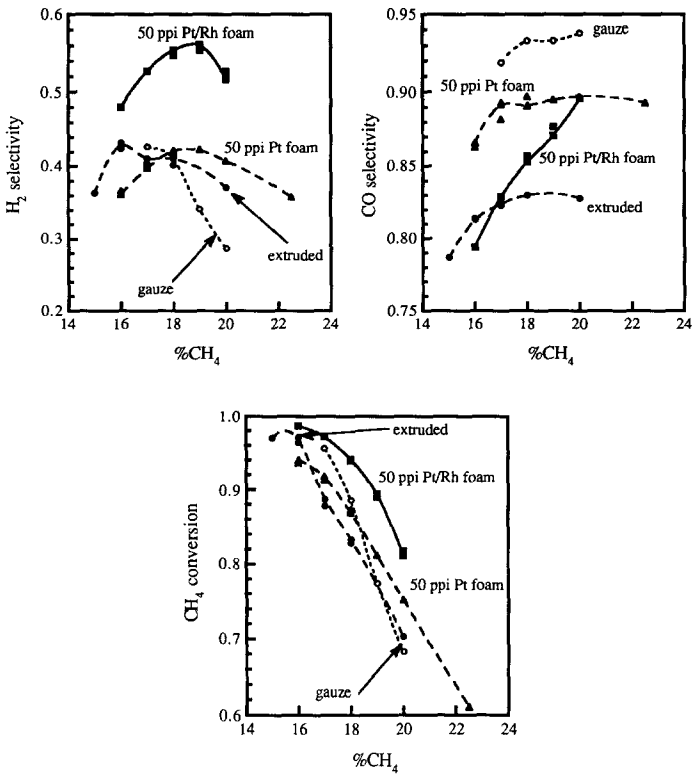

FIG. 5. Product selectivities and CH_4 conversion for the following samples: five layers of 40 mesh Pt-10% Rh gauze; a 7-mm long, 14-wt% Pt extruded monolith with 400 cells/in^2; a 7-mm long, 12-wt% Pt, 50-ppi foam monolith; and a 7-mm long, 9.9-wt% Pt and 9.9-wt% Rh, 50-ppi foam monolith. These experiments were all performed at 4 to 5 slpm total flow.

ppi Pt foam. Although not shown, an identical extruded monolith with a very low loading of Pt (about 0.1 wt%) gives a similar CO selectivity (~82%) but a much lower maximum H_2 selectivity (10 vs 45%) than the monolith with a high Pt loading. Similar results were observed for foam monoliths with relatively low metal loadings. Thus, the formation of H_2 occurs on the noble metal surface, not in the gas phase or on the catalyst support.

An additional observation in these experiments was that the ceramic monoliths maintained relatively large temperature gradients in the axial direction because of their lower thermal conductivity (relative to a metal gauze). As shown in the upper panel of Fig. 6, the upstream surface was generally significantly hotter than the downstream face of the catalyst. This suggests that most of the exothermic oxidation reactions are occurring on or near the front surface of the catalyst. With such high surface temperatures and, thus, significant rates of heat loss from the reactor, the observed axial temperature drops should be expected.

Activation and Deactivation

The effects of catalyst activation and deactivation were also examined by comparing the results for different gauze samples. SEM micrographs of gauzes having various catalytic activities are consistent with observations of catalysts used for HCN synthesis and NH_3 oxidation. In HCN synthe-

sis, the gauze wires undergo surface roughening during the first few hours of use. This roughening is accompanied by a significant change in the selectivity of the HCN synthesis catalyst (*20*).

For these methane to synthesis gas experiments, however, *the surface roughening of the gauze was not accompanied by an increase in selectivity*. A new gauze pack (5 to 10 layers) gave optimal adiabatic H_2 and CO selectivities of approximately 40 and 90%, respectively, with no reactor preheat. Although an activation period was not observed (steady state was achieved in a few minutes), some gauze catalysts did show a drastic decrease in activity and selectivity to synthesis gas after being exposed to very high temperatures (>1300°C) for a time of several hours or after being tested over a wide range of feed conditions. This decrease in activity was accompanied by a change from a faceted surface morphology to smoother, rounded surface structures and pits.

The supported catalyst samples showed no significant change in selectivity after operation for many hours at variable feeds and temperatures as high as 1300°C. However, SEM micrographs of new and used Pt foam catalysts showed a striking contrast in microstructure. The fresh catalysts contained polycrystalline structures with well-defined facets and characteristic dimensions on the order of 1 μm, while the used catalysts had rounded surface structures of similar characteristic dimensions.

To a good approximation, we believe that all of these catalysts are basically Pt metal surfaces. The loadings are sufficient to deposit uniform films ~1 μm thick on the Al_2O_3 or cordierite ceramics, and even if there were significant interactions with Pt, there should still be considerable metal surface remaining. The absence of deactivation and the close similarity of all the monoliths confirms this assumption, even though SEM showed that Pt formed large crystalline grains, thus exposing ceramic surfaces.

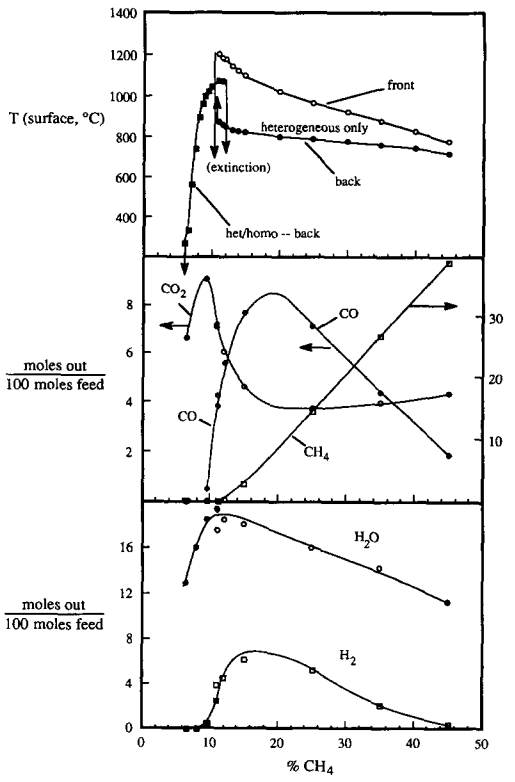

FIG. 6. Product compositions and surface temperatures (upstream and downstream ends) for a 7-mm long, 12-wt% Pt extruded monolith (400 cells/in^2) at 2.5 slpm total flow. The H_2 and CO selectivities are lower than those reported in previous experiments because the reactor was not insulated. A heterogeneous steady state reaction is maintained for rich (>12%) compositions, while at leaner compositions, a combination of heterogeneous and homogeneous reactions (a blue flame) is observed, with multiple ignited steady states for compositions between 10 and 12% CH_4.

Homogeneous Reactions and Multiple Steady States

For all of the experiments described in previous sections, a single steady state dominated by the heterogeneous reactions was observed. However, for feed compositions near the stoichiometric composition for total combustion, reaction (5), obvious homogeneous reactions (blue flames) and multiple steady states were observed, as shown in Fig. 6. For these experiments, the insulation around the quartz reactor tube was removed

and radiation shields were not used. If the reactor were well insulated, the highly exothermic reactions producing $CO_2 + H_2O$ would *melt the catalyst and the reactor tube* near the stoichiometric composition for this reaction (9.5% CH_4 in air). The upper panel shows the surface temperatures at the upstream and downstream ends of an extruded monolith. The lower panels show the measured product gas composition.

For rich feeds (>12% CH_4), only one ignited steady state exists; this is the same heterogeneous reaction autotherm observed in all of the previously described experiments. In this fuel rich regime, the front surface temperature exceeds the back temperature by 50 to 350°C, with the two temperatures approaching the same value at high feed CH_4 concentrations. This temperature maximum at the front end of the monolith is consistent with the fact that most of the reactions occur at this end of the monolith. Because the heat losses from the reactor tube are very high for this noninsulated experiment, the catalyst is hottest at the point where most of the reaction occurs.

As the feed concentration of CH_4 is decreased, the temperatures increase while the CH_4 conversion increases. The formation of H_2 and CO passes through a maximum and the rate of the temperature rise is even greater for leaner mixtures as more H_2O and CO_2 are formed. Note that the selectivities found here relative to previously shown data are lower; this results from a lower autothermal catalyst temperature for these non-insulated experiments.

As shown in the upper panel, below about 10% CH_4 the reactions at the front end of the monolith extinguish. At this point the hot reaction zone moves downstream as a transient lasting less than a minute until it reaches the back end of the monolith and a blue flame appears about 1 mm behind the monolith. Both homogeneous (flame) and heterogeneous reactions are now occurring. This second autotherm is stable to feed compositions up to 12% CH_4, giving two ignited states between 10 and 12%. In addition, this second autotherm is sustained until the CH_4 composition falls below 6%. As this lower limit is approached, the heterogeneous reaction gradually cools and the flame begins to stabilize further from the back of the monolith until it finally blows out. In this regime, the monolith acts as a flame holder until the mixture becomes too lean to maintain a stable homogeneous reaction.

DISCUSSION

These results provide several insights into the partial oxidation of CH_4 to synthesis gas. It is evident that this reaction system is governed by a combination of kinetic and transport effects. The reaction kinetics depend on the nature of the catalyst and the surface temperature, while transport of the gas species to the catalytic surface is a function of the catalyst geometry and flow velocity.

Although perfect (equilibrium) selectivities and conversions were not obtained in these experiments, the selectivity of the Pt catalysts to both H_2 and CO is surprisingly high. Because of the short residence times used in these experiments, the shift and reforming reactions do not play a significant role in determining the reactor selectivities and conversions.

In Table 1, we compare our measured S_{CO} and S_{H_2} from Fig. 2 at their optima with those predicted at chemical equilibrium of reactions (1) and (2). If these two reactions were at equilibrium at the measured temperatures, both S_{H_2} and CH_4 conversion would be much higher, while S_{CO} would be slightly lower. Thus, a reactor with longer residence times (probably 100 times longer than those used here) would allow for the shift and reforming reactions to occur, although additional preheat or a reactor design which recycles the generated heat (such as that described in Ref. (*2*)) would be needed to counter the endothermicity of the reforming reaction.

TABLE 1

Optimal Selectivities for Direct Oxidation of CH_4 in Air over the Foam Monolith from the Data Shown in Fig. 3

%CH_4 in air	Preheat (°C) → T(out, °C)	Observed			Shift equilibrium			Reform. equilibrium			Total equilibrium		
		S_{CO}	S_{H_2}	ΔCH_4 (%)	S_{CO}	S_{H_2}	ΔCH_4 (%)	S_{CO}	S_{H_2}	ΔCH_4 (%)	S_{CO}	S_{H_2}	ΔCH_4 (%)
19	25 → 1010	0.89	0.42	81	0.67	0.53	81	0.92	0.63	100	0.80	0.68	100
21	300 → 1020	0.92	0.53	83	0.75	0.61	83	0.93	0.70	100	0.85	0.75	100
23	460 → 1040	0.92	0.60	80	0.80	0.67	80	0.94	0.80	100	0.90	0.82	100

Note. The first three columns are the observed selectivities and CH_4 fractional conversions, the second three columns are the selectivities and conversions that would be obtained if the shift reaction (reaction 2) went to equilibrium, the third three columns are the selectivities and conversions that would be obtained if the reforming reaction (reaction 1) went to equilibrium, and the last three columns are the selectivities and conversions that would be obtained if all reactions went to equilibrium. All equilibria were calculated at the observed temperature of the product gases.

Although these experiments do not give the equilibrium yields of H_2 and CO reported in other work at much longer residence times, they show that both H_2 and CO are *primary products* of the direct oxidation of CH_4 over a Pt catalyst.

Reaction Steps

Traditionally, Pt has been used in hydrocarbon oxidation because of its tendency to *totally oxidize* all species. However, our results strongly suggest that H_2 and CO are formed as primary products in CH_4 oxidation because any secondary reactions such as methane steam reforming or water–gas shift are too slow.

Surface reactions which produce H_2 and CO occur in an oxygen-depleted environment, and the major surface species are probably adsorbed C or CH_x and H. The C reacts with oxygen to produce CO, which desorbs before being further oxidized to CO_2. Adsorbed H atoms may either combine to form H_2 which desorbs or react with oxygen to make adsorbed OH species, which then combine with additional adsorbed H atoms to form H_2O. Thus, H_2 and CO can be formed in the following reaction sequence:

$$CH_{4g} \rightarrow CH_{xs} + (4 - x)H_s \quad (10a)$$
$$2\,H_S \rightarrow H_{2g} \quad (10b)$$
$$O_{2g} \rightarrow 2\,O_s \quad (10c)$$
$$C_s + O_s \rightarrow CO_s \rightarrow CO_g. \quad (10d)$$

However, any reactions involving OH, such as

$$CH_{xs} + Os \rightarrow CH_{x-1,s} + OH_s \quad (11a)$$
$$H_s + O_s \rightarrow OH_s \quad (11b)$$
$$OH_s + H_s \rightarrow H_2O_g \quad (11c)$$
$$CO_s + O_s \rightarrow CO_{2g}, \quad (11d)$$

should all lead *almost inevitably* to H_2O and CO_2 because reverse reactions of these products are slow or thermodynamically unfavorable.

A CH_4 pyrolysis mechanism appears to be consistent with our observation that preheating improves partial oxidation selectivity. First, higher feed temperatures will increase the surface temperature and consequently decrease the surface coverage of O adatoms, thus decreasing reactions (11a–d). Second, high surface temperatures also increase the rate of H atom recombination and desorption of H_2, reaction (10b). Third, methane adsorption on Pt is known to be an activated process. From molecular beam experiments which examined meth-

ane chemisorption on Pt and Rh (*21–23*), it is known that CH_4 must overcome an activation energy barrier for chemisorption to occur. Apparently, methane chemisorption is produced by a combination of vibrationally and translationally excited modes. Stewart and Ehrlich (*23*) estimated an activation energy of 7 kcal/mole on Rh, asserting that vibrational energy alone was responsible for CH_4 chemisorption. In addition, experiments on Pt(111) which isolated the effect of incident translational energy showed that the barrier height for breaking the C-H bond by kinetic energy is 29 kcal/mole (*21*). Thus, the rate of reaction (10a) is accelerated exponentially by higher gas temperatures, which is consistent with the data in Fig. 2.

Kinetics

While many fundamental studies have evaluated the reaction kinetics of methane oxidation under fuel lean conditions at lower temperatures, the kinetics of these reactions have been examined less extensively at high temperatures (>800°C) and fuel-rich conditions.

Experiments on methane oxidation over a Pt foil at total pressures between 0.05 and 1.0 Torr for CH_4/O_2 ratios between 1/4 and 4/1 showed that $r_{CO} \gg r_{CO_2}$ above ~600°C (*11*). Production of H_2 and H_2O was not measured in those experiments. For a 2/1 CH_4/O_2 mixture, r_{CO_2} reaches a maximum at ~1000°C and then decreases, while r_{CO} continues to increase with temperature. Thus, S_{CO} is increased by operating at higher temperatures. These observations are supported by UHV studies of CO oxidation on Rh(111), Rh(100), and Pt(100) (*9, 10*) which showed that the CO oxidation reaction has a *negative activation energy* at high temperatures.

For the H_2–O_2–H_2O reaction system, the elementary reaction steps have been identified and reaction rate parameters have been determined using laser-induced fluorescence to monitor the formation of OH radicals during hydrogen oxidation and water decomposition at high surface temperatures. These results have been fit to a model based on the mechanism (*24*).

The kinetics of the water–gas shift reaction (*2*) and the steam reforming reaction (*3*) will also affect the composition of the product stream. These two reactions are carried out industrially over catalysts other than Pt, and therefore most kinetic studies have focused on different catalysts for these reactions. One exception is an analysis of the shift reaction over polycrystalline Pt wires at low pressures and 500 to 1500 *K* (*8*). This study found this reaction to be about an order of magnitude slower than the rate of methane oxidation at similar total pressures and surface temperatures.

Mass Transfer

As we have discussed previously (*16*), methane partial oxidation selectivity is strongly affected by the mass transfer rate. By increasing the linear velocity of the gases or choosing a catalyst geometry that gives thinner boundary layers, the selectivity of formation of H_2 and CO is enhanced. Such behavior is consistent with a series-parallel reaction scheme of partial oxidation. The above mechanism suggests that H_2 and CO are intermediates, with H_2O and CO_2 being the total oxidation products.

As outlined by Carberry (*25*), the selectivity of formation of partial oxidation products can be a strong function of the rate of mass transfer of reactants and products to and from the catalytic surface. The existence of thinner boundary layers essentially means that the concentration of the partial oxidation products in the gas near the surface is reduced, decreasing the rate of total oxidation of these species. Furthermore, the rate of formation of these partial oxidation products is mass transfer limited, so thinner boundary layers mean higher overall rates. The same reasoning applies if H_2O and CO_2 are formed in the boundary layer near the catalyst surface. Reducing the residence time of reactive species in this boundary layer will reduce the effect of reactions producing the total oxidation products.

Thus, because the direct oxidation of CH_4 is so fast, the mass-transfer rate must be high or H_2 and CO will react with O_2 to form the total oxidation products, reducing the partial oxidation selectivity and decreasing the amount of O_2 available to react with CH_4.

SUMMARY

We have shown that CH_4 can be oxidized directly to H_2 and CO over Pt monolith catalysts with surprisingly high selectivities for contact times of 10^{-2} to 10^{-4} sec. In these experiments, it appears evident that H_2 and CO are primary products of the *direct* oxidation of CH_4. Of special importance is the observation that H_2 can be formed directly by CH_4 oxidation on Pt with a selectivity of as high as 0.7.

Stoichiometry and thermodynamics of the CH_4–O_2 system suggest that perfect selectivities and complete conversion should be obtainable for a feed containing 30% CH_4 in air. Experiments using several different catalyst configurations demonstrate that the approach to this equilibrium is accelerated by operating at higher temperatures, by maximizing the rate of mass transfer through the boundary layer at the catalyst surface, and by using high metal loadings. Thus, a direct oxidation reactor should utilize a high flow velocity and a catalyst geometry which maximizes the rate of mass transfer through the boundary layer at the catalyst surface. In addition, the reactor should incorporate a design that recycles the generated heat so that high autothermal temperatures can be maintained. By optimizing the selectivity of direct formation of the partial oxidation products, the relatively long residence times required for steam reforming of the unreacted CH_4 can be reduced, requiring less catalyst and a much smaller reactor.

We also note that, even though mass transfer effects are significant, the kinetics of individual steps strongly influence selectivities. On Rh surfaces, the H_2 selectivity is much higher than on Pt, $S_{H_2} \geq 0.9$, and this is due primarily to the slower rate of hydrogen oxidation on Rh than on Pt as will be described in a later publication.

The short residence times used in these tests have allowed us to study this direct oxidation independent of the reforming and shift reactions. A better understanding of the factors that influence this partial oxidation selectivity should contribute to an improved understanding of the methane oxidation reactions and should lead to more efficient reactors.

ACKNOWLEDGMENT

The authors thank Dr. L. Campbell of Advanced Catalyst Systems, Inc., for preparing many of the catalyst samples used in these experiments.

REFERENCES

1. Korchnak, J. D., Dunster, M., and English, A., World Intellectual Property Organization, WO 90/06282 and WO 90/06297 (1990).
2. Blanks, R. F. Wittrig, T. S., and Peterson, D. A., *Chem. Eng. Sci.* **45,** 2407 (1990).
3. Dissanayake, D., Rosynek, M. P., Kharas, K. C. C., and Lunsford, J. H., *J. Catal.* **132,** 117 (1991).
4. Ashcroft, A. T., Cheetham, A. K., Foord, J. S., Green, M. L. H., Grey, C. P., Murrell, A. J., and Vernon, P. D. F., *Nature* **344,** 319 (1990).
5. Vernon, P. D. F., Green, M. L. H., Cheetham, A. K., and Ashcroft, A. T., *Catal. Lett.* **6,** 181 (1990).
6. Twigg, M. V. (Ed.), "*Catalyst Handbook.*" Wolfe Publishing, Ltd., London, 1989.
7. Satterfield, C. N., "*Heterogeneous Catalysis in Practice.*" McGraw–Hill, New York, 1980.
8. Blieszner, J. W., Ph.D. thesis, University of Minnesota, 1979.
9. Schwartz, S. B., Schmidt, L. D., and Fisher, G. B., *J. Phys. Chem.* **90,** 6194 (1986).
10. Schwartz, S. B., Ph.D. thesis, University of Minnesota, 1986.
11. Hasenberg, D., and Schmidt, L. D., *J. Catal.* **104,** 441 (1987).
12. Trimm, D. L., and Lam, C., *Chem. Eng. Sci.* **35,** 1405 (1980).
13. Firth, J. G., and Holland, H. B., *Trans. Faraday Soc.* **65,** 1121 (1969).
14. Otto, K., *Langmuir* **5,** 1364 (1989).
15. Griffin, T. A., and Pfefferle, L. D., *AIChE J.* **36,** 861 (1990).
16. Hickman, D. A., and Schmidt, L. D., submitted for publication.

17. Williams, W. R., Zhao, J., and Schmidt, L. D., *AIChE. J.* **37,** 641 (1991).
18. Lane, G. S., and Wolf, E. E., *J. Catal.* **113,** 144 (1988).
19. Yao, Y. Y., *J. Catal.* **87,** 152 (1984).
20. Pan, B. Y. K., *J. Catal.* **21,** 27 (1971).
21. Schoofs, G. R., Arumainayagam, C. R., McMaster, M. C., and Madix, R. J., *Surf. Sci.* **215,** 1 (1989).
22. Stewart, C. N., and Ehrlich, G., *Chem. Phys. Lett.* **16,** 203 (1972).
23. Stewart, C. N., and Ehrlich, G., *J. Chem. Phys.* **62,** 4672 (1975).
24. Williams, W. R., Marks, C. M., and Schmidt, L. D., *J. Phys. Chem.*, in press.
25. Carberry, J. J., "*Chemical and Catalytic Reaction Engineering.*" McGraw-Hill, New York, 1976.